

Visualizing demographic evolution using geographically inconsistent census data

Fabio Dias and Daniel Silver

Abstract—We propose a visual analytics system that enables the exploration evolutionary patterns in geographically inconsistent data, removing the need for harmonization of the geographical regions into a common geometry, a time consuming and error-prone process that is currently used in virtually all longitudinal analysis of geographical data. This work also includes incremental developments in the representation, clustering, and visual exploration of region-based geographical data. While we leverage the well known context of census data, our proposal is suitable for any region-based data. The method enables an easier identification and understanding of the demographic groups present in a city and their evolution over time. We present the feedback of experts in urban sciences and sociology, along with illustrative scenarios in the USA and Canada on the decennial censuses between 1970 and 2010.

1 INTRODUCTION

URBAN sciences are blooming thanks to a renewed interest in understanding and improving the urban environment. Visual analytics is following this trend, fueled by new public datasets that encompass progressively more of our daily lives [1]. There is no shortage of methods to explore mobility patterns [2], social media [1], traffic [3], and so on, providing experts, planners, policy makers, and the general population with deeper insights about their cities.

These new datasets usually contain GPS coordinates for the records, leading to *point-based* data. Combined with the corresponding timestamps, this data is easily suitable for longitudinal analysis. But most demographic datasets are *region-based*, where the measurements are associated with pre-defined regions, not only for an additional level of privacy protection, but because some measurements only make sense over a defined area. Census data is a classic example of this format, with datasets available from 1790 onward for the US [4]. Despite this unmatched temporal availability, longitudinal analyses of census data are often restricted in time, especially when smaller tabulation areas are considered, such as census tracts (CT) or dissemination areas, which evolve to reflect changes in population density, leading to geographic inconsistencies across time, and the traditional time-series based approach is no longer viable.

However, these analyses are necessary to understand the urban environment. Indeed, two different regions can have similar average income for a given year, while one is experiencing a process of economic improvement and the other one impoverishment. A single snapshot cannot be used to identify gentrification, migration, education changes, or any of the relevant processes that happen over time.

To overcome these inconsistencies, the traditional approach is the *geographical harmonization* of the data, the interpolation of the measurements into a common set of

regions [5], [6], [7], so that each variable can be represented using time-series. This is laborious work that inevitably introduces some amount of error [8], even when additional data is provided [9]. Nevertheless, this step is considered mandatory in the current literature: “(...) *tract-by-tract comparison is not possible unless data from 2000 is interpolated to 2010 boundaries (...)*” [10].

The main contribution of this application paper is an visualization-based alternative to the geographical harmonization, a combination of established graph based processing and information visualization techniques allowing tract-by-tract comparison, the identification and visualization of patterns of demographic evolution without geographic harmonization, effectively removing one of the most challenging problems in longitudinal demographic analysis. We also include illustrative scenarios and our prototype is available at <http://uoft.me/piccard>, including more than forty regions in the US and Canada. The source code is publicly available at <https://github.com/fabioasdias/piccard>.

2 RELATED WORK

Since our problem encompasses several fields, we divided this section into specific sub problems: *longitudinal demographic studies*, describing the traditional approach to perform longitudinal studies; *data representation*, exploring how evolving geographic data can be represented for processing; *Data clustering*, briefly reviewing existing clustering methods; and *cluster characterization*, exploring how the clusters can be visually summarized.

2.1 Longitudinal demographic studies

Census data is used not only to discover demographic patterns [11], but to correlate demographic characteristics to other measurements [12]. However, longitudinal studies are rare: “(...) One of the most challenging and fascinating areas in spatial statistics is the synthesis of spatial data collected at different spatial scales(...)” [13].

While CT level data is readily available for the US since 1910 [4], most studies consider the period between 1970

• F. Dias is with the Department of Mechanical & Industrial Engineering, University of Toronto, Toronto, ON, M5S 3G8.
E-mail: fabio.dias@utoronto.ca

• D. Silver is with the Department of Sociology, University of Toronto, Toronto, ON, M5S 2J4.
E-mail: dsilver@utsc.utoronto.ca

Manuscript received MMMM DD, YYYY; revised MMMM DD, YYYY.

73 and 2010, using pre-harmonized data [4], [5]. Despite the
 74 inherent errors [6], [8], this dataset became the standard
 75 source for longitudinal demographic data, with similar ef-
 76 forts appearing in other countries [7], [14], [15]. This result
 77 was significant for the field, but it also restricts the usable
 78 data, since new datasets need to be similarly processed.

79 Another option considers the use of grid data [10], [16],
 80 where small rectangular areas are used, in an approach
 81 similar to satellite imagery. Beyond the increased spatial ac-
 82 curacy, this approach does not require complex harmonization
 83 when new data is considered. However, demographic
 84 data is usually not available in this format, especially from
 85 older sources, and the conversion from tabulation areas can
 86 introduce significant errors.

87 In the proposed methodology, we avoid the harmo-
 88 nization by considering each measurement using its actual
 89 geographic region. It does not require the regions to be
 90 consistent across time because they are already represented
 91 as different entities.

92 **2.2 Data representation**

93 Most data is represented in tabular form, where the rows
 94 and columns have coherent definitions. For example, con-
 95 sider a table with rain measurements over time, with the
 96 rows representing different locations and the columns dif-
 97 ferent times. This representation can also be interpreted as
 98 a collection of time-series, one for each location. Geographic
 99 data followed this format, only including an additional field
 100 that describes the associated geographic area. Following the
 101 example, the data would now represent the amount of rain
 102 for a given region and time. As long each region remains
 103 the same, the data is coherent and can be interpreted again
 104 as a collection of time-series.

105 In the proposed method, we remove the requirement
 106 for consistency in the measurement regions by leveraging a
 107 graph-based representation, where each region in time cor-
 108 responds to a different node. Instead of a collection of time-
 109 series, the data is represented as a dynamic graph. Graph
 110 based representation of geographic information is fairly well
 111 explored in the literature, as a basis for topological methods
 112 for event detection [17], leveraging signal processing on
 113 graphs [18], [19] to find patterns and outliers [20], [21],
 114 [22]. Graphs are well suited to represent trajectories as
 115 well [2], [3], [23], allowing the use of graph visualization
 116 methods [24], [25].

117 Graphs were used to represent census data for clustering
 118 purposes before [21], [26], but these works did not explore
 119 temporal evolution, where graphs are particular powerful as
 120 they allow a natural representation of inconsistent regions,
 121 with both spatial and temporal connections. Note that there
 122 are other possible representations that have similar proper-
 123 ties, but we adopted graphs to allow the use of the existing
 124 literature and methods.

125 **2.3 Data clustering**

126 Data clustering is one of the elementary processes for data
 127 analysis, simplifying the data into a smaller number of
 128 homogeneous sets that can be interpreted in the same way.

While there is no shortage of contributions for this prob-
 129 lem [27], most applications still rely on k-means [28], [29]
 130 and, to a lesser extent, Self Organizing Maps [30], [31].

131 However, a method for geographic data analysis should
 132 not ignore the geographic component of the data. One
 133 straightforward option, for agglomerative methods [32], is
 134 to consider only nearby clusters for merging [33], which
 135 can also be done for k-means [34]. Alternatively, the spatial
 136 distance could be directly added to the inter-cluster met-
 137 ric [33] via a mixing parameter, which adds flexibility to the
 138 method, but introduces the problem of finding the correct
 139 application-dependent values.

140 Indeed, one crucial step in most clustering algorithms
 141 is the definition of the number of clusters. We sidestep
 142 this problem by considering hierarchical methods [35],
 143 where the result is not a partition of the data, but a tree
 144 of partitions. This approach is interesting for interactive
 145 methods, because it allows the user to change the number
 146 of displayed clusters with minimal processing. Since our
 147 data is represented as a graph, one option would be the
 148 watershed cuts algorithm [36], inspired by the well known
 149 image processing segmentation and equally prone to over
 150 segmentation. Considering that the processing time is also
 151 a relevant factor, we opted for an heuristic variation of
 152 the maximum weighted matching algorithm called *sorted*
 153 *maximal matching* [37], which merges clusters based on the
 154 weights of the edges between pairs of clusters.

156 **2.4 Cluster characterization**

157 Visually representing evolving spatial data is a challenging
 158 old problem [38], [39], [40], [41]. Most geographic data
 159 is naturally bi dimensional and maps work well in this
 160 case [41], [42], but the temporal dimension cannot be so nat-
 161 urally represented. One straightforward option is to lever-
 162 age tridimensional plots [43], [44], but this can lead to visual
 163 obstructions or scaling problems unless a tridimensional
 164 display device is used. Animation can also be explored in
 165 some specific cases [45], but it is not a general approach.
 166 Glyphs can also be used [46], [47], but this may lead to
 167 cluttering when many small regions are present. A simpler,
 168 well adopted, option is to display a map that corresponds
 169 to a subset of the temporal information, allowing the user
 170 to change the time with an associated control [1], [17], [20],
 171 [22]. Small multiples can be used [2], but only when there
 172 are few temporal snapshots. However, none of these options
 173 is suitable to represent many variables at the same time.

174 Using data clustering, we can represent the region's
 175 cluster instead of all the its variables [2], [20], [22]. While
 176 this simplifies the geographic portion of the visualization, it
 177 introduces the problem of how to summarize the contents of
 178 each cluster. One traditional approach is to use parallel coor-
 179 dinates plot [48], [49], [50], [51], but these they can get clut-
 180 tered representing similar clusters over several variables.
 181 Further, for demographic applications, the clusters are usu-
 182 ally strongly characterized by a small subset of values [29],
 183 [30]. Therefore, in the proposed method, we identify the
 184 variables that are most relevant to the characterization of
 185 each cluster. The distribution of values on that variable is
 186 then represented using a boxplot, a well known statistical
 187 plot displaying basic properties of the distributions.

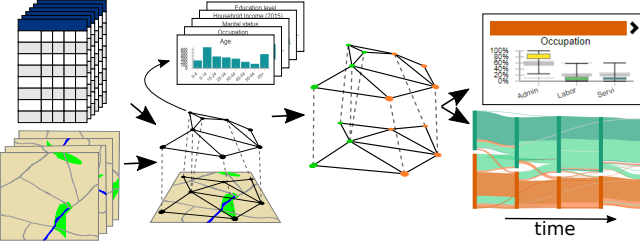


Fig. 1. Overview of the proposed method. A graph is generated combining the original census data, encoding the changing geographical information. The graph is partitioned into an hierarchy [37]. The characteristics and evolution of the clusters are then visually represented.

188 3 VISUALIZING THE DEMOGRAPHIC SPATIO- 189 TEMPORAL EVOLUTION

190 Beyond the objective of allowing the study of inconsistent
191 data, our method includes incremental developments in
192 most steps of the analysis, from data representation to the
193 visualization method for the clusters. Figure 1 presents an
194 overview of the processing steps of the proposed method.

195 3.1 Census methodology and data representation

196 Census data is disseminated in a tabulated form for aggre-
197 gation areas: whole country, state/province, metropolitan
198 region, and so on. To provide as much detail as possible, we
199 focus on the smallest region with available data: *census tracts*
200 (CT). They are usually defined to maintain the anonymity
201 of the population, leading to a population count in the
202 order of thousands in densely populated areas. Physical
203 barriers are usually adopted as borders, so these regions can
204 change because of new roads, construction or removal of
205 high density buildings, and so on. Some census entities also
206 consider demographic characteristics, aiming to establish
207 the CTs as a cohesive unit. Therefore, CTs are the least
208 geographically stable tabulation area.

209 Each CT is associated with a series of variables, with
210 counts derived from the census questionnaires, covering
211 several aspects of the demographic characteristics of the
212 population. Some questions allow for multiple choices
213 or open answers, that are then tabulated into the most
214 frequent categories. Since the census is often used to
215 direct government initiatives, which variables are mea-
216 sured/disseminated is dependent on administrative inter-
217 ests, the general understanding of the population, and cur-
218 rent customs. For instance, income is disseminated with a
219 finer tabulation in the lower portion than on the higher.

220 To match these variables over time and allow for direct
221 comparison across different census years, we aggregated
222 similar ones (e.g. White, Black, Asian, Other) into *aspects*
223 (e.g. Race), encoding the distribution of that facet of the
224 population. In this convention, we refer to the composing parts
225 of an aspect as a *part* or the traditional *variable*. Internally,
226 the aspects are represented using normalized histograms.
227 This normalized representation is crucial for the comparison
228 between inconsistent regions.

229 In our graph based representation, each CT of each
230 census year is represented as a node, and edges are placed
231 between nodes if the corresponding CTs share geographic

232 borders in the same year. Further, edges are placed be-
233 tween nodes if the corresponding CTs belong to sequential
234 years and there is geographical overlap between them. This
235 approach leads to a single graph representing the whole
236 spatio-temporal space of the data. Our objective then be-
237 comes to identify partitions of this graph such that the
238 nodes of each partition are more similar between themselves
239 than to the other nodes. This representation is not the only
240 option, nor unique, but it allows the use of existing graph-
241 based methods for the other steps.

242 3.2 Geographic content clustering

243 To partition the graph we must first establish a distance
244 function between the nodes, measuring the data similarity.
245 This similarity is then associated with the edges, leading
246 to a weighted dynamic graph. Every node has a collection
247 of histograms, each representing the distribution of certain
248 aspect in the population.

249 Let $G = (V, E)$ be a graph, where $V = \{v_1, v_2, \dots, v_n\}$
250 is the set of nodes and $E = \{(v_i, v_j), i \neq j \text{ and } i, j \in [1, n]\}$
251 is the set of edges. A function H associates each node to a
252 set of K histograms. We define the distance D between two
253 nodes v_i and v_j as:

$$D(v_i, v_j) = \sum_{k \in [1, K]} w_k d(H_k(v_i), H_k(v_j)) \quad (1)$$

254 where d is a distance metric between histograms and w is
255 a sequence of non-negative weights associated with each
256 aspect, $\sum_{k \in [1, K]} w_k = 1$. While any histogram metric can
257 be used, we adopted a euclidean distance between the
258 vectors, because it led to reasonable results with reduced
259 computational cost. Therefore the distance between two
260 nodes is defined as the weighted average distance between
261 its associated histograms, where the weights can be adjusted
262 by the user.

263 Once the distances are associated to the edges, we use
264 watershed cuts [36] to create an initial clustering, which
265 is then refined into a hierarchy using the Sorted Maximal
266 Matching (SMM) [37] with median linkage. The initial wa-
267 tershed step is performed to create an initial clustering and
268 reduce the running time of the SMM. For completeness, we
269 briefly review this method, but we refer the reader to the
270 original paper [37] for more details, including a complete
271 performance evaluation using several metrics.

272 We included two application-specific parameters: the
273 maximum number of clusters to be shown and a distance
274 threshold. Contrarily to the original SMM, which merges all
275 clusters in all steps, we only merge two clusters where the
276 distance is above the threshold after we reach the maximum
277 number of displayed clusters. Without this restriction, sig-
278 nificantly different clusters would be merged early, leading
279 to increased intra cluster variance and the disappearance of
280 small outlier regions. Further, after the maximum number
281 of clusters is reached, we create one step of the hierarchy
282 for each merge, leading to a binary partition tree. In this
283 structure we can directly access a result with an arbitrary
284 number of clusters.

285 Each resulting cluster is contiguous in the graph. This
286 means that two similar, but non-contiguous, sets of CTs
287 will be classified into two different clusters, which can

be counter-intuitive. To overcome this issue, we *augment* the graph with two new edges per node from a nearest neighbors graph [52] using only the distances between the histograms. These edges connect nodes with similar content, if they are not already connected, providing a path for the algorithm to group similar nodes. Theoretically, adding more of these content based edges could be used to decrease the impact of the spatio-temporal edges, controlling the balance between content and topology in the result. In practice, the effect is dependent on the data itself, and the results are not consistent, or predictable, across different cities. We fixed it at two edges because it was the lowest number that empirically led to consistent clusters, but we believe that this idea warrants further investigation, as an alternative to mixing parameters in the distance metric [33].

3.3 Cluster characterization and variable relevance

The composition of each cluster is determined by simple statistical measures, considering each aspect separately. We compute the minimum, maximum, median, 25%, and 75% quantiles for each part of each aspect for all clusters in the hierarchy. While interpreting these values is more complex than interpreting just the average, they provide far more information about the underlying distribution.

We also use these statistical measurements to discover what characterizes each cluster, that is, what makes it different from the others. We define the *relevance* of a part of an aspect based on the distance between the interquartile ranges (IQR) of the clusters in the same hierarchical level. If the IQRs overlap for all clusters, that variable is not relevant to the characterization of the cluster, but if the IQRs are distant, it means that this specific range of values is something that only occurs in this cluster.

3.4 Clusters and trajectories

While the partition of the data into different clusters helps the user to understand what groups exist and where they are, we are also interested in the evolution of these groups. We introduce the concept of *trajectories*, composed by regions classified into the same sequence of clusters over the considered period. This enables direct access to regions that evolved in the same manner. While the interface provides access to data by individual census tract, the trajectories are the main unit of exploration in this work.

3.5 Colors

As illustrated by Figure 3 and further explored in the next subsection, our proposed interface heavily relies on color to express cluster-related information. We adopted this convention because colors can be used in all our visual tools in a coherent manner. However, this also introduced significant challenges. The first is the limit on the number of clusters that can be visually represented. We limited the number of clusters to eight because this was the largest number of colors that we could reliably use, derived from the 8-class Dark2 set from ColorBrewer [53].

While we can reasonably limit the number of clusters, there are far more possible trajectories. And the color associated with each trajectory should bear some resemblance

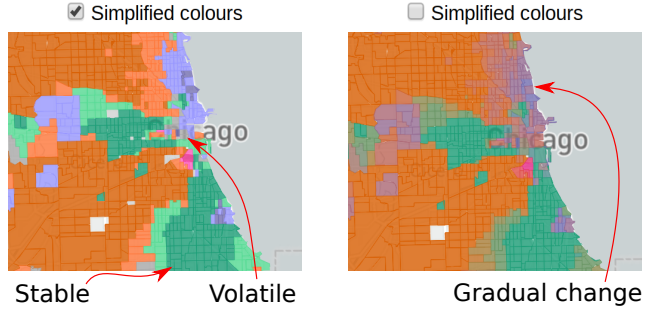


Fig. 2. Different color schemes for Chicago with four clusters. Left: simplified, right: average color.

to the clusters included in it. Therefore, we were left with a conundrum: *Should we associate each trajectory with a unique color, which the user probably cannot distinguish, or should we use a reduced set of colors and associate the same color to different trajectories?* Since there are advantages and disadvantages for each of those options, we adopted both. The user can control which color policy is used via a checkbox in the configuration panel, on the top left of the interface.

By default, the interface adopts a simplified color scheme, where a trajectory is painted in the same color of a cluster if the regions were associated to that cluster for *all* times; in a slightly less saturated version of that color if the regions were associated to that cluster for *the simple majority* of the time, and gray otherwise. In this mode, the colors will mostly represent stability, immediately identifying the regions that were consistently associated with each cluster. It also easily identifies volatile regions, painted gray.

When this simplified color scheme is disabled, each trajectory will be painted using the average of the colors of the involved clusters, in the LAB color space. In this mode, the map becomes more similar to a heatmap, where stronger presence of a color indicates more temporal affinity to the cluster. Volatile regions will also tend to be displayed in gray, as the average of three or more colors.

While both approaches will use more than eight colors, in practice this is not as significant because most cities can be explained using less than eight clusters. In fact, articles in the literature usually employ from two to five, which are fairly stable across time. For the more dynamic scenarios, user interaction can be used to alleviate the shortcomings of both approaches.

3.6 User interface

The initial interface is illustrated in Figure 3. Since demographic data can be nuanced, with intricate interconnections, we decided against validating the interface using a synthetic dataset, considering instead data from the Chicago region between 1970 and 2010, using previous published studies as corroboration. This region is known for its entrenched racial divide and the emergence of a '*young urban*' population with a higher education level [29], [30]. More details about this dataset are presented in Section 4.

The configuration panel, on top left in Figure 3, displays which aspects were used and their weights (following Equation 1). It also includes other configuration options that can be altered without re-processing the data, such as the

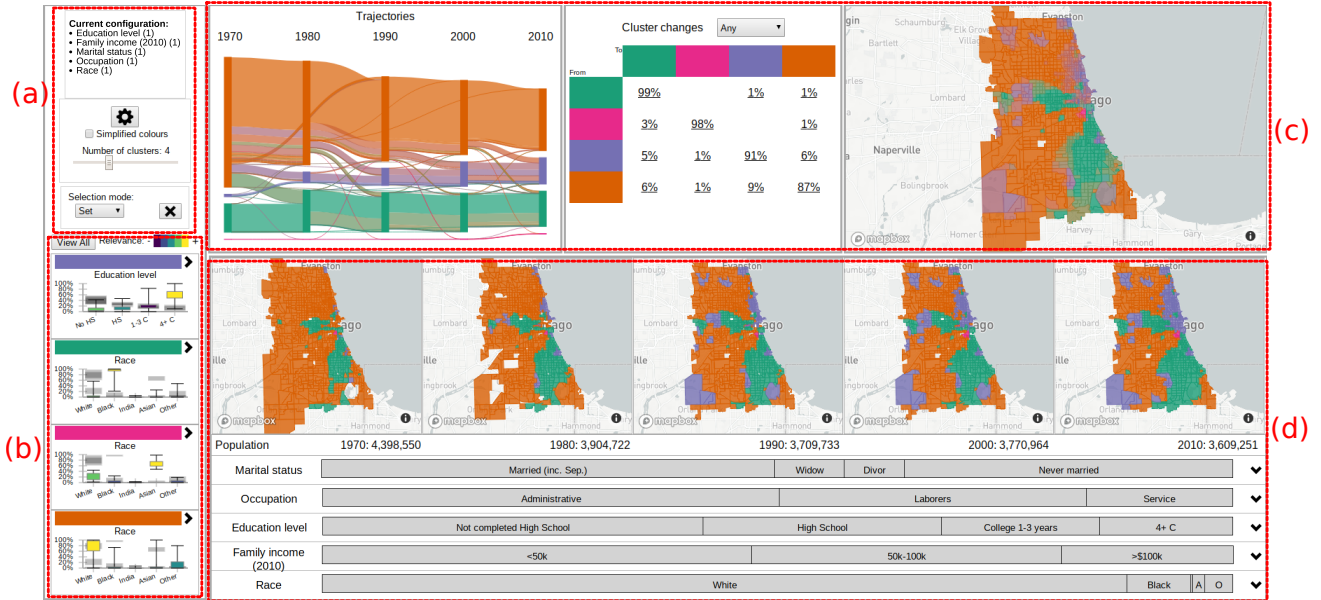


Fig. 3. Initial interface of our method showing the demographic evolution of Chicago. (a): Configuration panel with the current clustering parameters and controls. (b): Cluster overview illustrating the most relevant aspect for each cluster. (c): Trajectories overview and the general evolution of the population, geographical information, and how it changed. (d): Details of the selected trajectories, including precise geographic locations, population numbers, and the composition of the aspects.

number of clusters and the color option. The gear button allows access to the other configuration options that do require further processing, such as changing location, aspects, and weights. This panel also includes the configuration of the selection mode for the trajectories, which allows the user to set, add, or remove the next selected trajectories to the current selection. This feature enables the analysis of complex sets of trajectories.

The cluster overview panel, on the bottom left in Figure 3, displays a brief summary of each cluster, based on the distance between the IQRs, as detailed in Section 3.3. The *View all* button opens a new panel where all aspects are represented, while the chevron at the side of the color lets the user expand each cluster separately. While the standard approach to represent cluster characteristics is to use parallel coordinates [50], [51], this representation occupies screen space proportional to the number of variables and can get cluttered with a higher number of clusters, or when the clusters are not well defined for multiple variables. To save space and leverage the familiarity scientists have with statistical tools, we opted to use boxplots to properly convey the distribution of each variable in the current cluster. However, a simple boxplot would not include information about the other clusters, forcing the user to mentally compare them to find what is relevant.

We adopt an *enhanced* version of the traditional boxplot, which includes the minimum, maximum, 25% and 75% quantiles for the current cluster, but also the IQRs for the other clusters, in slightly larger and faded black rectangles. We also color the current IQR according to its relevance. While there might be some degree of similarity between the color schema for relevance and for trajectory identification, none of the experts consulted reported confusion. Indeed, one expert reported confusion regarding the grey rectangles that represent the IQRs for other distributions when they

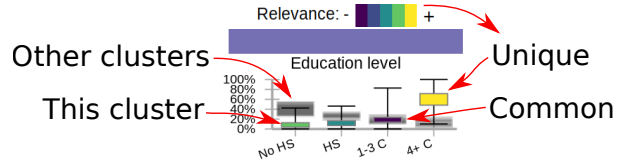


Fig. 4. Enhanced boxplot of the clusters' characteristics allows a quick comparison to the other clusters.

are not colored; when that variable is not relevant to the characterization of the cluster. These simple changes allow the user to easily understand the composition of the cluster and how it relates to the others. Violin plots [54] could also be used, providing more information about the shape of the distribution, but with increased potential for obstructing the representation of the other clusters.

For instance, the boxplot that summarizes the purple cluster illustrated in Figure 3, detailed on Figure 4, illustrates that this cluster is best defined by the proportion of the population with four or more years of college. The user can quickly see that this is relevant because the corresponding IQR is colored with the highest relevance present in the legend. It is also clear that, while this cluster includes CTs that have between 10% to 90% of people in this variable, approximately, half of them have about 60% of the population with four or more years of college. Since all the other IQRs are well separated, this is a defining characteristic of this cluster. Conversely, the proportion of the population with one to three years of college is not relevant, as indicated by black fill in the rectangle representing the IQR of this cluster, in overlapping position with the rectangles of the other clusters. By clicking on the colored bar above the boxplot, the user can select all trajectories that contain this cluster at any point in time.

449 The other clusters identified on Figure 3 correspond to
 450 higher concentration of people that identify as Black in
 451 the green cluster, people that identify as "Asian, Hawaiian,
 452 other pacific islander" in the pink cluster, and people that
 453 identify as White in the orange cluster. From these plots,
 454 it is clear that the city is indeed racially divided [29], with
 455 several CTs that are almost exclusively occupied by people
 456 of the same racial category.

457 The trajectories overview aims to convey basic information
 458 about the trajectories, where they are, and what changes are involved. This is done using three sub panels.
 459 The first, on the left, contains a Sankey diagram illustrating
 460 the evolution of the clusters over time. The widths are
 461 proportional to the population involved, the colors follow
 462 a policy detailed in Section 3.5. A stacked graph could also
 463 be used to represent the proportions of each cluster [20] with
 464 less clutter, since the transitions between clusters would
 465 not be represented. However, this is only viable if more
 466 temporal steps are available, making the plot smoother.
 467 Another option to remove clutter is to remove portions
 468 of this plot when trajectories are selected, but this would
 469 change the layout and compromise the user's mental map.
 470

471 In our example in Figure 3, the total population of
 472 Chicago is decreasing. Additionally, the orange and green
 473 clusters contain most of the population and are fairly stable
 474 over time. The pink cluster is small and mostly stable.
 475 The purple cluster is increasing, mostly by incorporating
 476 areas that were previously orange. Since the purple group
 477 corresponds to the emergent 'young urban' group, this corrobates
 478 the findings of Delmelle [29], [30]. This diagram
 479 can also be used to select specific trajectories, by clicking on
 480 the bands, or all trajectories that contain a specific cluster at
 481 a specific time, by clicking on the rectangles.

482 In the next panel, illustrated in the top middle of Figure 3, is a transition matrix between the clusters. It indicates
 483 the percentage of the population whose area changed be-
 484 tween each pair of clusters. This kind of table can be found
 485 in the related literature [29], so it is familiar to the advanced
 486 users. It not only informs the proportional changes, but
 487 allows the selection of the corresponding trajectories for
 488 further analysis.

489 Contrary to the trajectories plot, this representation is
 490 more Markovian, where only the current and next state are
 491 considered. This panel also enables easier access to trajec-
 492 tories with specific changes, by clicking on the corresponding
 493 percentage values. The combo box allows the user to refine
 494 the transitions, from 'Any', which includes all transitions be-
 495 tween years, to specific transitions, to changes from the first
 496 year to the last year. In this example, approximately 99%
 497 of the population in areas classified as green were also in
 498 areas classified as green in the next year, while 1% changed
 499 to purple at some point and another 1% to orange. The total
 500 is over 100% due to rounding errors. Regions changed from
 501 the orange to the green cluster for 6% of its population, 1%
 502 to pink, and 9% to purple. This further corroborates the fact
 503 that most of the growth of the purple cluster came from the
 504 orange cluster. Additionally, the lack of transitions is also
 505 relevant, for instance, no CT changed from majority of Black
 506 population (green) to Asian population (pink), and no CT
 507 with significant Asian population had significant increase
 508 in education levels (purple).

509 The panel in the top right of Figure 3 is a map of
 510 the region under analysis, summarizing the geographical
 511 evolution of the clusters over time. The colors are derived
 512 from the clusters involved in each trajectory as detailed in
 513 Section 3.5, which are consistent across the linked views.
 514

515 The bottom part of the interface contains the details for
 516 the selected trajectories, or for the whole city if nothing
 517 is selected, as illustrated in Figure 3. This panel contains
 518 two main regions: the small multiple maps, depicting the
 519 clusters at each year, and the stacked bar plots that sum-
 520 marize the overall composition of these regions. Some finer
 521 localization information is lost using small multiples, such
 522 as small border changes, but that information is available
 523 at the larger map. All the maps are linked with synchro-
 524 nized navigation, and the use of small multiples allows the
 525 exploration of each temporal census individually, and its
 526 comparison to the others, with minimal interaction.
 527

528 In this example, the maps show the transition from
 529 orange to green and purple in several regions over time.
 530 Clicking on a region in these maps will bring up a new
 531 panel with the original census data of this specific region.
 532 The actual population numbers are below the maps, and
 533 they confirm the notion provided by the Sankey diagram
 534 that the total population is indeed decreasing.
 535

536 Each aspect is represented by a stacked bar plot, where
 537 the width of each rectangle corresponds to the average
 538 percentage of that variable over the considered period. We
 539 chose stacked bar plots to represent the composition of the
 540 regions because they can accurately and succinctly inform
 541 the proportions of each aspect, without any interaction.
 542 In this case, about half of the people in Chicago in the
 543 considered period are married, and the percentage that are
 544 Widowers or Divorced is roughly similar. About half of
 545 the population work in Administrative jobs, a third never
 546 completed high-school, approximately half have gross fam-
 547 ily income below 50,000USD per year. The vast majority
 548 identify as white. Placing the mouse over one of the bars
 549 will open a small panel with the temporal evolution of that
 550 specific variable, and clicking on the chevron on the right
 551 side expands the corresponding aspect, showing details
 552 of the temporal evolution of each variable and also the
 553 corresponding IQRs for the whole city.
 554

4 ILLUSTRATIVE SCENARIOS

555 We used decennial census data from the United States [4]
 556 and Canada¹, tabulated by CTs, from 1970 to 2010. The
 557 prototype allows access to 40 regions, 28 in the US and 12
 558 in Canada. Due to the high number of CTs, New York City
 559 was split into its boroughs.

560 We used five aspects for the USA: Education level,
 561 Family income, Marital status, Occupation, and Race; and
 562 seven for Canada: Age, Education level, Home language,
 563 Household Income, Marital status, Occupation, Place of
 564 birth, and Religion. While our method does not require
 565 geographic harmonization, it requires matching variables
 566 over time. The supplementary material contains the details
 567 of which census columns were used for each aspect. Income
 568 is slightly inaccurate, even though we did correct for official
 569

570 1. <http://datacentre.chass.utoronto.ca/census/>

567 inflation. We grouped the original ranges into three larger
 568 ranges, but they do not match precisely.

569 4.1 Chicago

570 We selected a region loosely following the administrative
 571 borders. The demographic composition is well explored in
 572 the literature, with reports of racial divide and gentrification
 573 [29], [30], [55]. While the definition of gentrification is
 574 still unclear and out of the scope of this paper, we associate
 575 gentrification with higher education and income levels.

576 The initial state of the prototype is illustrated in Figure 3,
 577 and its findings are explained in Section 3.6, where the
 578 racial divide is clear. Starting from this initial state, the
 579 specific workflow used to identify the existence and details
 580 of the gentrification process are illustrated in Figure 5. For
 581 the users, the first step is to identify the compositions of
 582 each cluster from the boxplots, so orange is associated with
 583 majority of White population, green with majority Black,
 584 and purple with higher proportion of four years of college
 585 or more (high education level). The expanded version of the
 586 boxplots for the purple cluster shows a higher income level
 587 and majority of occupations in administrative jobs, therefore
 588 the purple cluster identifies gentrified regions.

589 The trajectories plot illustrates the process of gentri-
 590 fication, progressively absorbing regions from the orange
 591 cluster (White). This corroborates results from the literature
 592 reporting that Black neighborhoods are less likely to gen-
 593 trify [55]. Moreover, this process is unlikely to be reversed,
 594 as indicated by the limited number of trajectories leaving the
 595 purple stream. Next, we select the region that is gentrified
 596 in 2010, by clicking on the corresponding rectangle in the
 597 trajectories plot, updating the information on the maps and
 598 the details portion of the interface.

599 The corresponding CTs are highlighted in the maps,
 600 where the spatial pattern is clear, corresponding exactly
 601 to previous findings in the literature [55]. Further, we can
 602 also identify the regions that gentrified earlier, with an
 603 stronger purple hue, compared to newer regions, where the
 604 orange and green colors are still present. This also indicates
 605 from which clusters they belonged before gentrifying. In the
 606 details portion of the interface, the order of the aspects was
 607 updated to reflect the order of relevance considering only
 608 the selected region. The most relevant aspect is the Educa-
 609 tion, specifically "Four or more years of college", illustrated
 610 in the rightmost portion of Figure 5, which is increasing for
 611 the whole city (grey band), but faster and to a higher level
 612 in this region (black band). Indeed, while the IQR for the
 613 city goes from 11% to 45%, the IQR for this region goes
 614 from 55% to 77%. However, there are portions of this region
 615 with significantly lower or higher proportions, as indicated
 616 by the dotted black lines representing the minimum and
 617 maximum for the selected region.

618 4.2 Toronto

619 We considered a region that is approximately the adminis-
 620 trative border of the current city of Toronto and all seven
 621 available aspects with equal weights. The results are sum-
 622 marized in Figure 6, considering eight clusters.

623 The population with low percentage of University
 624 degrees is represented in orange, mostly anglophone popula-
 625 tion in green, Asian immigrants in yellow, high percentage

626 of income in the highest bracket in purple, high percentage
 627 of Jewish people in light green and brown, high percentage
 628 of Eastern Non-Christian religion in pink, and high concen-
 629 tration of single people in dark gray. From the trajectories
 630 plot, we can see that Toronto is more dynamic than Chicago,
 631 with one cluster constantly shrinking. In the 1970s, the city
 632 was divided into four clusters: low number of university
 633 degrees, Jewish population, majority anglophones, and high
 634 income. Interestingly, the more recent clusters that absorbed
 635 regions from the orange cluster have similar education
 636 profiles and are differentiated by other aspects. In this sense,
 637 the city is growing diverse, changing from a common low
 638 education profile to a higher level of education with more
 639 diversity in religion (pink) and immigration (yellow).

640 Indeed, the influx of Asian population is visible starting
 641 in the 1980s and building thereafter, leading to the yellow
 642 and pink clusters. While both include a high percentage of
 643 people born in Asia, the pink is more defined by religion,
 644 with low percentage of university degrees, and contains the
 645 lowest percentage of people in the highest income bracket
 646 for these clusters; the yellow is less defined by religion,
 647 and has higher education and income, geographically cor-
 648 responding to the Markham region, known for its Chinese
 649 population. A similar division also happens for the two
 650 Jewish clusters, where the light green cluster has lower
 651 education and income levels than the brown cluster. The
 652 purple cluster of high income is somewhat stable. This
 653 cluster includes the Bridle Path neighborhood, known for
 654 its wealthy population, until 2011. In 2011 it was classified
 655 into the yellow cluster of Asian immigration, since about
 656 35% of the population for this CT were then born in Asia.
 657 The income distribution did not change, with 85% of the
 658 population with an income of 90k CAD or more.

659 The most significant indicator of Toronto's dynamism is
 660 the presence of grey regions on the simplified color map;
 661 representing regions associated to three or more clusters
 662 over this five census period. Using the 'Add' mode for
 663 the trajectory selection, we select their trajectories, and a
 664 subset of the details is illustrated in Figure 7. These regions
 665 account for about 5% of Toronto's population. The whole
 666 region was classified into the orange cluster in 1971 (low
 667 level of university degrees). By 1991, most of the region was
 668 classified into the green cluster, representing anglophone
 669 population, mostly Canadian born, with a higher level of
 670 education. As the corresponding plot indicates, this trend in
 671 increasing education is city-wide, but this region has people
 672 with better education than most.

673 In 2001, the purple cluster of high income annexes neigh-
 674 borhood parts of the volatile region, and the Asian born pop-
 675 ulation increases sharply, as illustrated by the appear-
 676 ance of the yellow cluster. This cluster indicates well educated,
 677 higher income, and about 30%-50% Asian born population.
 678 By 2011, the yellow cluster increased considerably, annex-
 679 ing parts of the high income purple cluster, including the
 680 neighboring Bridle Path area.

681 4.3 Los Angeles

682 We selected a region around the metropolitan area of Los
 683 Angeles (LA), following urban density. The summary of
 684 the results using all aspects with equal weights and eight

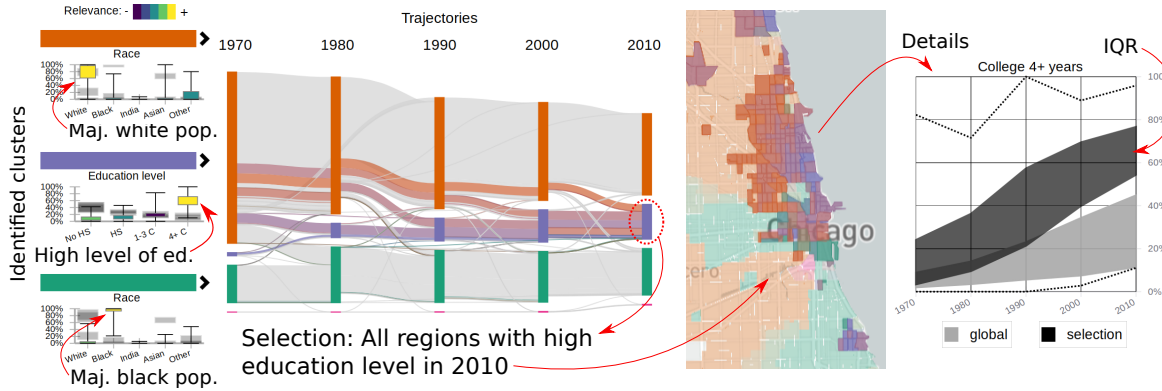


Fig. 5. Workflow to discover gentrification in Chicago: the purple cluster corresponds to high education / income. Its population is increasing over time, absorbing from the majority White cluster (orange). By selecting the purple cluster in 2010, the region is highlighted in the maps. The proportion of people with 4+ years of college is increasing in the whole city (grey IQRs), but significantly more in this region (black).

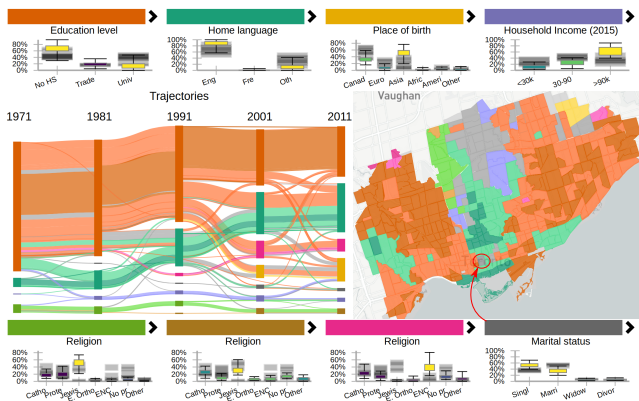


Fig. 6. Clustering results for Toronto, with eight clusters, including clusters representing Jewish population, high and low income, low education, and Asian immigration.

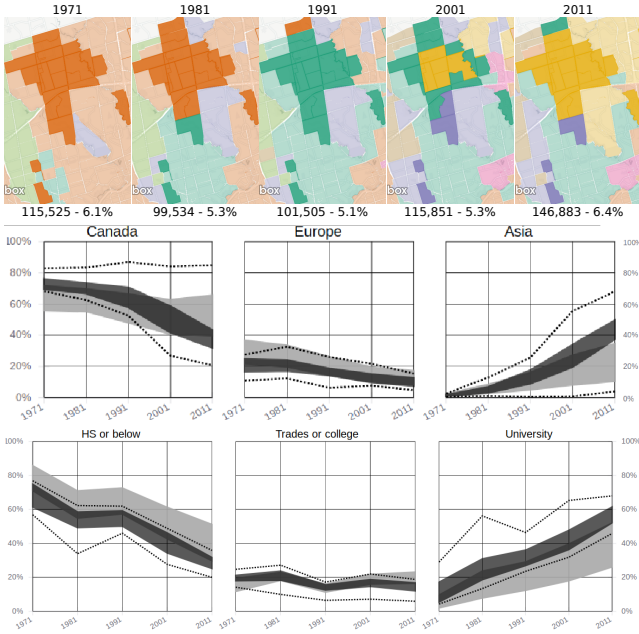


Fig. 7. Details for some regions of Toronto that were classified into 3 or more clusters over time.

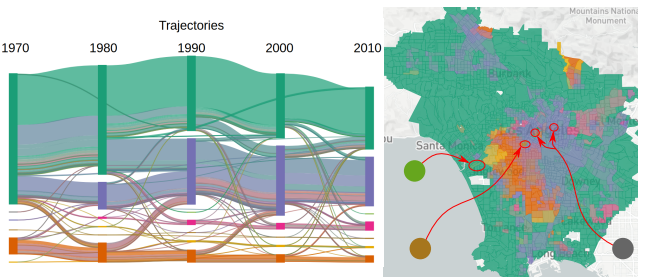


Fig. 8. Result for Los Angeles with 8 clusters, including three small and ephemeral clusters. Cluster characterization is displayed in Figure 9.

clusters is illustrated in Figure 8. The full statistical description of the clusters is illustrated in Figure 9, where the most relevant aspect of each cluster is highlighted. From the trajectories plot, we can see that there is a large but shrinking cluster, depicted in green, one increasing cluster in purple, an almost constant orange cluster, a smaller but increasing pink cluster, and three other small clusters. The corresponding map illustrates where these clusters are located, and that they are somewhat geographically stable, with some movement between the green, orange, and purple clusters.

From Figure 9, we can see that the green cluster is characterized by a high percentage of White population, low percentage of population in the lowest income bracket, mostly administrative occupations, and about 30% of the population with four or more years of college. The orange cluster is characterized by a high percentage of Black population, with few people in the highest range of income and education. The purple cluster corresponds to a high concentration of "Other" in race, which includes Hispanic for this dataset, high concentration of Laborers, and low education and income. The pink cluster contains a high percentage of Asian population and about 30% of the population with four or more years of college. The light green cluster contains very few people in the lower income bracket, mostly White population, with the highest percentage of population with four or more years of college, working administrative jobs, and a high concentration of singles. The yellow cluster represents Black population, with higher level of education and income, mostly working administrative jobs. The brown

714 cluster represent a majority of single population, working
 715 administrative jobs with mostly low income. The dark gray
 716 cluster is characterized by all its population in the lowest
 717 income bracket, low education level, with a majority of
 718 White population. Since the extremes in the boxplots of
 719 the grey cluster are not significantly different, we can also
 720 surmise that this cluster is either small or homogeneous.

721 The green, orange, and purple clusters present a significant
 722 intra-cluster variance in most variables, as indicated
 723 by extreme whiskers of the boxplots. While fifty percent of
 724 the CTs in the green cluster have between 20% and 40%
 725 of people in the lowest income bracket, that cluster also
 726 includes CTs where none and all the population belongs to
 727 that bracket. This might indicate that this cluster represents
 728 different groups of people that are not different enough to be
 729 separated at this level of the hierarchy. Conversely, the light
 730 green, brown, and dark gray clusters are different enough
 731 to be separated into their own clusters at this level, despite
 732 being small and ephemeral, including only a few CTs.

733 The orange area in the map in Figure 8 presents move-
 734 ment, indicated by the presence of green and purple tones
 735 mixed with the orange, which may warrant further explora-
 736 tion. By clicking on the orange bar above the boxplot,
 737 we select all trajectories that contain the orange cluster.
 738 The corresponding details are illustrated in Figure 10. This
 739 shows a location change, where the orange cluster is pro-
 740 gressively replaced by the purple cluster on its east side, and
 741 in turn expanding to the west. Interestingly, the population
 742 increased, the racial profile changed, but the distribution of
 743 income was reasonably stable, with a higher amount of the
 744 population in the lowest income range and very few people
 745 in the highest income range. Indeed, the income difference
 746 is significant when compared to the city-wide distribution.

747 A portion of this region is classified into the green cluster
 748 in 2010, indicating a majority white population. To further
 749 understand that change, we clear the current selection,
 750 and select all regions that changed from orange in 1970
 751 to green in 2010, using the transition matrix. A portion of
 752 the resulting region, near the Florence-Graham region, is
 753 depicted in Figure 11, along with the temporal evolution of
 754 Race. Despite this difference, the other aspects are similar
 755 to the ones from the region in Figure 10, with slightly
 756 lower income and education profiles. While the racial aspect
 757 changed considerably, the economic and educational aspects
 758 stayed the same.

759 While Toronto is more dynamic than Los Angeles, pos-
 760 sibly due to size differences, the volatile regions shown in
 761 Figure 7 did not change as quickly or dramatically as the
 762 ones shown in Figure 11, which involved twice as many
 763 people. We found this trend to be related to the countries
 764 themselves, Canadian cities have larger areas undergoing
 765 slow, gradual changes, whereas American cities have more
 766 general stability, but quicker changes in smaller scales. The
 767 supplementary material contains brief summaries of all the
 768 regions accessible in this prototype.

769 5 EXPERT FEEDBACK

770 To assess the proposed method, we contacted academic
 771 and industry experts in sociology and urban sciences. We
 772 focused our inquiries on the utility of the prototype, and if

773 they found anything interesting on the data using it. The
 774 supplementary material contains the communication with
 775 five experts, verbatim, identified from A to E.

776 Their overall response was positive, mentioning that the
 777 prototype allows them to analyze census data without the
 778 additional work of obtaining and cleaning the data (A, B,
 779 E), and it allows the inclusion of geographic visual analysis
 780 tools in their research process (D). It enables the users to
 781 tell different stories about neighborhoods/cities and their
 782 changes (A), visualize the relationship between key urban
 783 variables over time (D), offering a quick way to identify
 784 particular neighborhoods that one may be interested in
 785 studying more in depth around a particular issue or effi-
 786 ciently understanding the context of an area (E). Indeed,
 787 the experts identified gentrification processes in Manhattan
 788 (B) and Dallas (E), reinforced a hypothesis for occupational
 789 clustering (D), and highlighted how the method can be used
 790 to compare neighborhoods and cities (A). In summary, the
 791 proposed methodology can be a viable alternative for the
 792 visual analytics of evolving demographic data.

793 The interface was "easy to navigate" (B), but it was also
 794 considered "overwhelming" (A), "intimidating" (E), and
 795 "tricky to interpret" (C), possible side-effects of our effort to
 796 increase representational accuracy, where we avoided using
 797 simplified representation or labels. Identifying clusters by
 798 their most relevant variables was welcome, but the overlap
 799 of information from different clusters in the boxplot was "a
 800 bit confusing" (C) when color was not present. Further, most
 801 clusters can be sufficiently characterized using only the most
 802 relevant aspect, but this is not generally true.

803 While the map of trajectories was mentioned as a "good
 804 summary map", how it related to the clustering method was
 805 unclear (C). The methods includes different options on how
 806 the colors are used, but both are sub optimal since reliably
 807 representing several distinct entities using colors is humanly
 808 unfeasible. Indeed, the number of distinguishable colors
 809 was a significant constraint, we found indications that more
 810 clusters should be used in some cases, even if eight clusters
 811 is more than what is traditionally considered in these anal-
 812 yses. Conversely, increasing the number of clusters would
 813 also complicate the interpretation of the results.

814 The experts also mentioned the poor responsiveness
 815 of the method when changes in the clustering parameters
 816 required server-side processing (B,D). Indeed, the current
 817 implementation can take a few minutes to cluster regions
 818 with high number of CTs, like Los Angeles or Brooklyn.
 819 Server-processing reduced the amount of data transferred
 820 to client, but it might increase the response time under
 821 load. We implemented a cache policy that greatly improved
 822 the performance, but fully pre-processing the results is not
 823 practical due to size of the parameter space.

824 Most of the experts demonstrated interest in using our
 825 method in their research (A, B, D, E), aiming to use the
 826 census data as a backdrop for other datasets, providing
 827 demographic context. They also mentioned the need to
 828 export subsets of data, plots, and maps to be used in reports
 829 and publications (C, D, E). More importantly, while these
 830 experts were aware that our method does not perform
 831 geographic harmonization, none of them mention it. We
 832 did not specifically ask if this difference led to unexpected
 833 results, but rather if they found interesting insights. Most

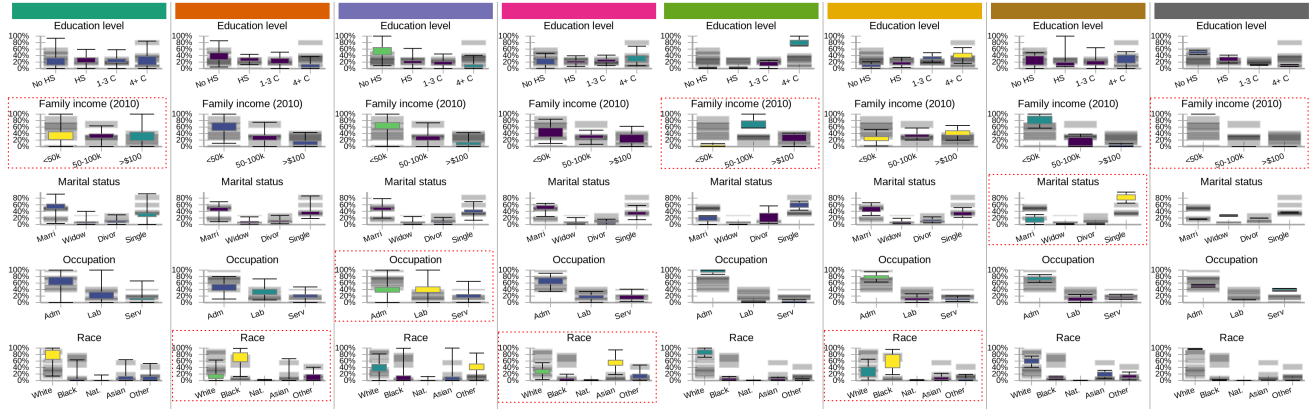


Fig. 9. Full characterization of the eight clusters found for LA. The red rectangles indicate the most relevant aspects for each cluster.

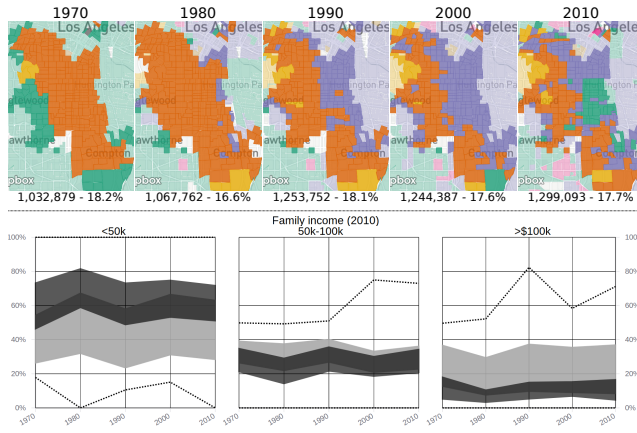


Fig. 10. Top: Geographic changes in the majority Black population cluster (orange) and Laborers cluster (green). Bottom: Income evolution for this region (black) and the whole city (gray).

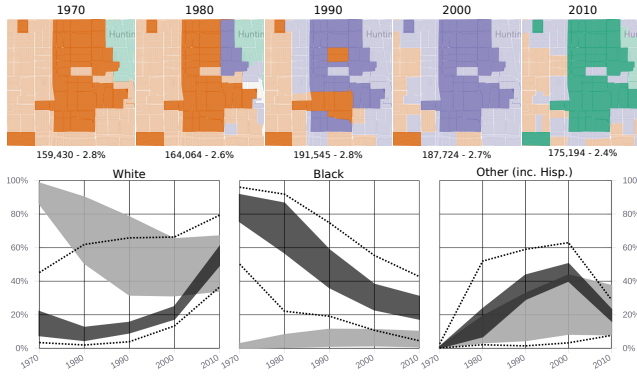


Fig. 11. Details for a volatile region contained in the area of Figure 10. This region went from Black to Hispanic to White.

834 experts found phenomena corroborated by the specialized
835 literature, indicating that our methodology produces equivalent
836 results, with a fraction of the effort. We interpret the
837 fact that most of them were interested in the next steps as
838 confirmation of the accuracy of the method.

839 6 DISCUSSION AND LIMITATIONS

840 Our objective was to leverage a graph based data representation and visualization methods for the exploration of
841

842 geographically inconsistent region-based data. While we
843 successfully replicated and corroborated results from the
844 literature, this method still has significant limitations.

845 Removing the need for geographical harmonization
846 greatly reduces the amount of work necessary to explore
847 demographic data, but the method still requires consistent
848 variables across the years. Matching the variables can be
849 trivial for some aspects (Age), but challenging for others
850 (Income). The divulged income ranges vary over time and
851 the actual values change due to inflation. Some variables
852 were not considered in earlier censuses, such as Race in
853 Canada, or Hispanic population in the USA, hampering its
854 use when they are available. Since this is only a prototype,
855 we matched few aspects, but a proper demographic analysis
856 would benefit from all available information.

857 While using one small map for each year leads to an
858 easier visualization that does not require interaction, it does
859 not scale if more than five or six years are considered. In
860 this case, it might be interesting to replace the larger map
861 considering each year individually, along with a temporal
862 control for navigation. Indeed, including more years would
863 likely lead to a stronger mixture of colors in the trajectory
864 map, leading to a predominantly grey hue.

865 The limitation on the number of displayed clusters be-
866 cause of the limited number of distinguishable colors was
867 significant. While increasing the number of clusters would
868 further complicate an already complex analysis, it might be
869 warranted for some regions. Color is a fundamental and
870 intuitive tool for information representation that can be
871 coherently used across different plots, so we opted to use
872 it, even if in a limited way. With eight colors, there was
873 overlap between some clusters, the relevance gradient, and
874 the color combination.

875 Another limitation is the lack of control on how much the
876 geographical information will impact the clustering result.
877 While the adopted method met our needs for this work,
878 a configurable control would add another dimension to
879 the exploration, allowing for more intra-cluster variance
880 to obtain more ‘compact’ clusters. We explored changing
881 the number of content based augmented edges, but this
882 proved to be unreliable and hard to interpret. The *ClustGeo*
883 method [33] can be a viable option for this, allowing a graph
884 based input and a hierarchical output, combined using a
885 single mixing parameter. Alternatively, one could cluster the

886 changes [56] instead of the stable states.

887 There are also technological limitations, such as memory
 888 use on the visualization client. To allow for changes on the
 889 CTs over the years, we use a geographic file that contains
 890 all possible intersections, which can grow rather large if the
 891 original city was expansive and contained several CTs, like
 892 NYC or LA. However, the most significant technological
 893 limitation relates to parameters that are not immediately
 894 interactive, such as the clustering configuration. Since the
 895 clustering is computationally expensive and performed on
 896 the server, which allows for cached results, some changes
 897 can take a few minutes to be considered, removing any
 898 possibility of a continuous exploration.

899 Indeed, the cognitive load on the user is already sig-
 900 nificant, as we compromised simplicity for accuracy. While
 901 other works labelled the clusters, as 'young urban', 'strug-
 902 gling', and so on [29], [30], we show the statistical charac-
 903 teristics of the clusters, which are harder to interpret, as the
 904 data may have subtle nuances that labels would otherwise
 905 hide. This also led to a crowded interface, mitigated some-
 906 what the use of pop-up panels and collapsible sections. For
 907 some cities, especially if they are small and stable, the panels
 908 can appear redundant, but each provide a different way to
 909 interact with the information that can ease the exploration
 910 process for larger and dynamic cities.

911 7 CONCLUSION

912 Our objective was to allow for the exploration of census data
 913 without geographical harmonization, an original alternative
 914 to a challenging and error-prone process. Our method was
 915 able to corroborate previous findings from the specialized
 916 literature, with an increased level of detail due to our data
 917 representation and visualization choices. The feedback from
 918 experts was positive and most of them were able to extract
 919 insight from the prototype and demonstrated interest in
 920 using it on their research efforts. Indeed, the experts also
 921 demonstrated further interest in similar tools, indicating
 922 that visual analytics methods can be valuable in this field.

923 ACKNOWLEDGEMENTS

924 This research was supported by a University of Toronto
 925 Connaught Global Challenge grant and is part of the Ur-
 926 ban Genome Project. The authors thank Cary Wu, Ethan
 927 Fosse, Fernando Caldern Figueroa, Patrick Adler, and James
 928 Murdoch for their expert opinions; Mark S. Fox, Robert M.
 929 Wright, Ultan Byrne, Matti Siemiatycki, Shauna Brail, and
 930 Richard Florida for general guidance and support; and the
 931 anonymous reviewers for their constructive comments.

932 REFERENCES

- 933 [1] W. Chen, Z. Huang, F. Wu, M. Zhu, H. Guan, and R. Maciejewski,
 "Vaud: A visual analysis approach for exploring spatio-temporal
 urban data," *IEEE Transactions on Visualization & Computer Graphics*, no. 1, pp. 1–1, 2017.
- 934 [2] T. Von Landesberger, F. Brodkorb, P. Roskosch, N. Andrienko,
 G. Andrienko, and A. Kerren, "Mobilitygraphs: Visual analysis
 of mass mobility dynamics via spatio-temporal graphs and clus-
 tering," *IEEE transactions on visualization and computer graphics*, vol. 22, no. 1, pp. 11–20, 2016.
- [3] W. Chen, F. Guo, and F.-Y. Wang, "A survey of traffic data vis-
 ualization," *IEEE Transactions on Intelligent Transportation Systems*, vol. 16, no. 6, pp. 2970–2984, 2015.
- [4] S. Manson, J. Schroeder, D. V. Riper, and S. Ruggles. (2017) Ipums national historical geographic information system: Version 12.0 [database]. Minneapolis: University of Minnesota. [Online]. Available: <http://doi.org/10.18128/D050.V12.0>
- [5] J. R. Logan, Z. Xu, and B. J. Stults, "Interpolating us decennial
 census tract data from as early as 1970 to 2010: A longitudinal
 tract database," *The Professional Geographer*, vol. 66, no. 3, pp. 412–
 420, 2014.
- [6] E. Hallisey, E. Tai, A. Berens, G. Wilt, L. Peipins, B. Lewis, S. Graham,
 B. Flanagan, and N. B. Lunsford, "Transforming geographic
 scale: a comparison of combined population and areal weighting
 to other interpolation methods," *International Journal of Health
 Geographics*, vol. 16, no. 1, p. 29, Aug 2017.
- [7] J. Allen and Z. Taylor, "A new tool for neighbourhood
 change research: The canadian longitudinal census tract
 database, 19712016," *The Canadian Geographer / Le Géographe
 canadien*, vol. 0, no. 0, 2018. [Online]. Available: <https://onlinelibrary.wiley.com/doi/abs/10.1111/cag.12467>
- [8] J. R. Logan, B. J. Stults, and Z. Xu, "Validating population esti-
 mates for harmonized census tract data, 2000–2010," *Annals of the
 American Association of Geographers*, vol. 106, no. 5, pp. 1013–1029,
 2016.
- [9] C. L. Eicher and C. A. Brewer, "Dasymetric mapping and areal
 interpolation: Implementation and evaluation," *Cartography and
 Geographic Information Science*, vol. 28, no. 2, pp. 125–138, 2001.
- [10] A. Dmowska, T. F. Stepinski, and P. Netzel, "Comprehensive
 framework for visualizing and analyzing spatio-temporal dynam-
 ics of racial diversity in the entire united states," *PLOS ONE*, vol. 12, no. 3, pp. 1–20, 03 2017.
- [11] G. Firebaugh and C. R. Farrell, "Still large, but narrowing:
 The sizable decline in racial neighborhood inequality in
 metropolitan america, 1980–2010," *Demography*, vol. 53, no. 1, pp.
 139–164, Feb 2016. [Online]. Available: <https://doi.org/10.1007/s13524-015-0447-5>
- [12] A. V. Diez-Roux, F. J. Nieto, C. Muntaner, H. A. Tyroler, G. W.
 Comstock, E. Shahar, L. S. Cooper, R. L. Watson, and M. Szklo,
 "Neighborhood environments and coronary heart disease: a mul-
 tilevel analysis," *American journal of epidemiology*, vol. 146, no. 1,
 pp. 48–63, 1997.
- [13] C. A. Gotway and L. J. Young, "Combining incompatible spatial
 data," *Journal of the American Statistical Association*, vol. 97, no. 458,
 pp. 632–648, 2002.
- [14] X. Liu, Y. Song, K. Wu, J. Wang, D. Li, and Y. Long, "Understand-
 ing urban china with open data," *Cities*, vol. 47, pp. 53 – 61, 2015,
 current Research on Cities (CRoC).
- [15] A. C.-D. Lee and C. Rinner, "Visualizing urban social change
 with self-organizing maps: Toronto neighbourhoods, 1996–2006,"
 Habitat International, vol. 45, pp. 92–98, 2015.
- [16] A. Dmowska and T. F. Stepinski, "Spatial approach to analyzing
 dynamics of racial diversity in large u.s. cities: 199020002010,"
 Computers, Environment and Urban Systems, vol. 68, pp. 89
 – 96, 2018. [Online]. Available: <http://www.sciencedirect.com/science/article/pii/S019897151730371X>
- [17] H. Doraiswamy, N. Ferreira, T. Damoulas, J. Freire, and C. T. Silva,
 "Using topological analysis to support event-guided exploration
 in urban data," *IEEE Transactions on Visualization and Computer
 Graphics*, vol. 20, no. 12, pp. 2634–2643, Dec 2014.
- [18] D. I. Shuman, S. K. Narang, P. Frossard, A. Ortega, and P. Vand-
 derghenst, "The emerging field of signal processing on graphs:
 Extending high-dimensional data analysis to networks and other
 irregular domains," *IEEE Signal Processing Magazine*, vol. 30, no. 3,
 pp. 83–98, 2013.
- [19] A. Sandryhaila and J. M. Moura, "Discrete signal processing on
 graphs," *IEEE transactions on signal processing*, vol. 61, no. 7, pp.
 1644–1656, 2013.
- [20] P. Valdivia, F. Dias, F. Petronetto, C. T. Silva, and L. G. Nonato,
 "Wavelet-based visualization of time-varying data on graphs,"
 in *2015 IEEE Conference on Visual Analytics Science and Technology
 (VAST)*, Oct 2015, pp. 1–8.
- [21] F. Dias and L. G. Nonato, "Some operators from mathematical
 morphology for the visual analysis of georeferenced data," in
 *Workshop on Visual Analytics, Information Visualization and Scientific
 Visualization - SIBGRAPI*, 2015.

- 1018 [22] A. Dal Col, P. Valdivia, F. Petronetto, F. Dias, C. T. Silva, and L. G.
 1019 Nonato, "Wavelet-based visual analysis of dynamic networks,"
 1020 *IEEE Transactions on Visualization and Computer Graphics*, vol. PP,
 1021 no. 99, pp. 1–1, 2018.
- 1022 [23] X. Huang, Y. Zhao, C. Ma, J. Yang, X. Ye, and C. Zhang, "Traj-
 1023 graph: A graph-based visual analytics approach to studying urban
 1024 network centralities using taxi trajectory data," *IEEE Transactions*
 1025 *on Visualization and Computer Graphics*, vol. 22, no. 1, pp. 160–169,
 1026 Jan 2016.
- 1027 [24] C. Vehlow, F. Beck, and D. Weiskopf, "The State of the Art in Visu-
 1028 alizing Group Structures in Graphs," in *Eurographics Conference on*
 1029 *Visualization (EuroVis) - STARS*, R. Borgo, F. Ganovelli, and I. Viola,
 1030 Eds. The Eurographics Association, 2015.
- 1031 [25] F. Beck, M. Burch, S. Diehl, and D. Weiskopf, "The State of the Art
 1032 in Visualizing Dynamic Graphs," in *EuroVis - STARS*, R. Borgo,
 1033 R. Maciejewski, and I. Viola, Eds. The Eurographics Association,
 1034 2014.
- 1035 [26] T. Setiadi, A. Pranolo, M. Aziz, S. Mardiyanto, B. Hendrajaya, and
 1036 Munir, "A model of geographic information system using graph
 1037 clustering methods," in *2017 3rd International Conference on Science*
 1038 *in Information Technology (ICSTech)*, Oct 2017, pp. 727–731.
- 1039 [27] A. Fahad, N. Alshatri, Z. Tari, A. Alamri, I. Khalil, A. Y. Zomaya,
 1040 S. Foufou, and A. Bouras, "A survey of clustering algorithms for
 1041 big data: Taxonomy and empirical analysis," *IEEE Transactions on*
 1042 *Emerging Topics in Computing*, vol. 2, no. 3, pp. 267–279, sep 2014.
 1043 [Online]. Available: <https://doi.org/10.1109/tetc.2014.2330519>
- 1044 [28] A. K. Jain, "Data clustering: 50 years beyond k-means," *Pattern*
 1045 *recognition letters*, vol. 31, no. 8, pp. 651–666, 2010.
- 1046 [29] E. C. Delmelle, "Mapping the dna of urban neighborhoods: Clus-
 1047 tering longitudinal sequences of neighborhood socioeconomic
 1048 change," *Annals of the American Association of Geographers*, vol. 106,
 1049 no. 1, pp. 36–56, 2016.
- 1050 [30] ———, "Differentiating pathways of neighborhood change in 50
 1051 u.s. metropolitan areas," *Environment and Planning A: Economy and*
 1052 *Space*, vol. 49, no. 10, pp. 2402–2424, 2017.
- 1053 [31] C. Ling and E. C. Delmelle, "Classifying multidimensional tra-
 1054 jectories of neighbourhood change: a self-organizing map and k-
 1055 means approach," *Annals of GIS*, vol. 22, no. 3, pp. 173–186, 2016.
- 1056 [32] J. Han, M. Kamber, and A. K. Tung, "Spatial clustering methods in
 1057 data mining," *Geographic data mining and knowledge discovery*, pp.
 1058 188–217, 2001.
- 1059 [33] M. Chavent, V. Kuentz-Simonet, A. Labenne, and J. Saracco,
 1060 "Clustgeo: an r package for hierarchical clustering with spatial
 1061 constraints," *Computational Statistics*, pp. 1–24, 2017.
- 1062 [34] S. Soor, A. Challa, S. Danda, B. D. Sagar, and L. Najman, "Extending
 1063 k-means to preserve spatial connectivity," 2018.
- 1064 [35] P. Soille and L. Najman, "On morphological hierarchical rep-
 1065 resentations for image processing and spatial data clustering,"
 1066 in *Applications of Discrete Geometry and Mathematical Morphology*.
 Springer, 2012, pp. 43–67.
- 1067 [36] J. Cousty, G. Bertrand, L. Najman, and M. Couperie, "Watershed
 1068 cuts: Minimum spanning forests and the drop of water principle,"
 1069 *IEEE Transactions on Pattern Analysis and Machine Intelligence*,
 1070 vol. 31, no. 8, pp. 1362–1374, Aug 2009.
- 1071 [37] M. D. Dias, M. R. Mansour, F. Dias, F. Petronetto, C. T. Silva,
 1072 and L. G. Nonato, "A hierarchical network simplification via non-
 1073 negative matrix factorization," in *2017 30th SIBGRAPI Conference*
 1074 *on Graphics, Patterns and Images (SIBGRAPI)*, Oct 2017, pp. 119–126.
- 1075 [38] M. Monmonier, "Strategies for the visualization of geographic
 1076 time-series data," *Cartographica: The International Journal for Geo-*
 1077 *graphic Information and Geovisualization*, vol. 27, no. 1, pp. 30–45,
 1079 1990.
- 1080 [39] N. Andrienko, G. Andrienko, and P. Gatalsky, "Exploratory spatio-
 1081 temporal visualization: an analytical review," *Journal of Visual*
 1082 *Languages & Computing*, vol. 14, no. 6, pp. 503–541, 2003.
- 1083 [40] N. Ferreira, "Visual analytics techniques for exploration of spa-
 1084 tiotemporal data," Ph.D. dissertation, Polytechnic Institute of New
 1085 York University, 2015.
- 1086 [41] Y. Zheng, W. Wu, Y. Chen, H. Qu, and L. M. Ni, "Visual analytics
 1087 in urban computing: An overview," *IEEE Transactions on Big Data*,
 1088 vol. 2, no. 3, pp. 276–296, Sept 2016.
- 1089 [42] M. O. Ward, G. Grinstein, and D. Keim, *Interactive data visual-
 1090 ization: foundations, techniques, and applications*. AK Peters/CRC
 1091 Press, 2015.
- 1092 [43] G. Andrienko, N. Andrienko, H. Schumann, and C. Tominski,
 1093 "Visualization of trajectory attributes in space-time cube and
 1094 trajectory wall," in *Cartography from Pole to Pole*. Springer, 2014,
 1095 pp. 157–163.
- [44] C. Tominski and H.-J. Schulz, "The Great Wall of Space-Time,"
 1096 in *Vision, Modeling and Visualization*, M. Goesele, T. Grosch,
 1097 H. Theisel, K. Toennies, and B. Preim, Eds. The Eurographics
 1098 Association, 2012.
- [45] S. Buschmann, M. Trapp, and J. Döllner, "Real-time animated
 1099 visualization of massive air-traffic trajectories," in *Cyberworlds*
 1100 (*CW*), 2014 International Conference on. IEEE, 2014, pp. 174–181.
- [46] D. Seebacher, J. Häußler, M. Hundt, M. Stein, H. Müller, U. Engelke,
 1101 and D. Keim, "Visual analysis of spatio-temporal event pre-
 1102 dictions: Investigating the spread dynamics of invasive species,"
 1103 in *2017 IEEE Visualization Conference (VIS)*, 2017.
- [47] G. Andrienko, N. Andrienko, G. Fuchs, and J. Wood, "Revealing
 1104 patterns and trends of mass mobility through spatial and temporal
 1105 abstraction of origin-destination movement data," *IEEE Transac-
 1106 tions on Visualization and Computer Graphics*, vol. 23, no. 9, pp. 2120–
 1107 2136, Sept 2017.
- [48] N. Ferreira, M. Lage, H. Doraiswamy, H. Vo, L. Wilson, H. Werner,
 1108 M. Park, and C. Silva, "Urbane: A 3d framework to support data
 1109 driven decision making in urban development," in *Visual Analytics*
 1110 *Science and Technology (VAST)*, 2015 IEEE Conference on. IEEE, 2015,
 1111 pp. 97–104.
- [49] M. Li, Z. Bao, T. Sellis, S. Yan, and R. Zhang, "Homeseeker:
 1112 A visual analytics system of real estate data," *Journal of Visual*
 1113 *Languages & Computing*, vol. 45, pp. 1 – 16, 2018.
- [50] J. Johansson, P. Ljung, M. Jern, and M. Cooper, "Revealing struc-
 1114 ture within clustered parallel coordinates displays," in *Information*
 1115 *Visualization, 2005. INFOVIS 2005. IEEE Symposium on*. IEEE, 2005,
 1116 pp. 125–132.
- [51] D. Guo, J. Chen, A. M. MacEachren, and K. Liao, "A visualization
 1117 system for space-time and multivariate patterns (vis-stamp),"
 1118 *IEEE transactions on visualization and computer graphics*, vol. 12,
 1119 no. 6, pp. 1461–1474, 2006.
- [52] F. Pedregosa, G. Varoquaux, A. Gramfort, V. Michel, B. Thirion,
 1120 O. Grisel, M. Blondel, P. Prettenhofer, R. Weiss, V. Dubourg,
 1121 J. Vanderplas, A. Passos, D. Cournapeau, M. Brucher, M. Perrot,
 1122 and E. Duchesnay, "Scikit-learn: Machine learning in Python,"
 1123 *Journal of Machine Learning Research*, vol. 12, pp. 2825–2830, 2011.
- [53] M. Harrower and C. A. Brewer, "Colorbrewer.org: An online tool
 1124 for selecting colour schemes for maps," *The Cartographic Journal*,
 1125 vol. 40, no. 1, pp. 27–37, 2003.
- [54] J. L. Hintze and R. D. Nelson, "Violin plots: a box plot-density
 1126 trace synergism," *The American Statistician*, vol. 52, no. 2, pp. 181–
 1127 184, 1998.
- [55] J. Hwang and R. J. Sampson, "Divergent pathways of gentrification:
 1128 Racial inequality and the social order of renewal in chicago
 1129 neighborhoods," *American Sociological Review*, vol. 79, no. 4, pp.
 1130 726–751, 2014.
- [56] J. Bian, D. Tian, Y. Tang, and D. Tao, "A survey on trajectory
 1131 clustering analysis," *arXiv preprint arXiv:1802.06971*, 2018.